Volumetric image analysis of pulsed non-thermal plasma produced by microwave

Y. Ikeda* and J.K. Soriano

i-Lab., Inc. KIBC #213, 5-5-2 Minotima-Minami Kobe, 65-0047 Japan
* Correspondent author: yuji@i-lab.net

Keywords: Microwave, Ignition, Plasma Temperature, Volumetric Plasma, High Speed Images

ABSTRACT

We have been developing microwave pulsed mode ignition system using 2.45 GHz microwaves. This technology has shown improvements in the lean combustion limit and fuel efficiency using a real engine with propane using a microwave discharged igniter (MDI). However, the MDI's expensive parts are a major drawback when compared to common igniters. For practicality, we shifted to a more economical flat spiral igniter to generate plasma enabling stable and sustained non-equilibrium plasma in the atmosphere. Incorporating semiconductor elements, we miniaturized the microwave generator system, enhancing compactness and increasing its efficiency. Initial plasma was generated by the partial energy from the microwaves (1 mJ) and the sustained plasma was maintained in the atmosphere by the rest of the microwave's energy. We varied long to short-pulsed modes, changed microwave pulse widths, increasing repetition rates which affecting plasma volume and stability. Our findings highlight the significance of microwave input patterns and the transition from thermal to non-equilibrium plasma. Future discussions should focus on the ignition mechanisms of various fuels and the transition from plasma source to initialization region. Our work contributes to the understanding and practical application of non-thermal plasma in combustion systems.

1. Introduction

Non-thermal plasma has been utilized in various basic research and applications(Bulat et al., 2019; Cheng et al., 2021; Hwang et al., 2016; S. Zhang et al., 2021), including surface treatment of materials(Akdoğan & Şirin, 2021), pharmaceuticals and medical applications (Akdoğan & Şirin, 2021), waste and gas treatment (Ong et al., 2022; Trinh et al., 2022). Recently, in the field of combustion, the nanosecond pulsed discharge method, which uses a high-current and high-voltage power supply for electrical discharge, has garnered significant attention (Dumitrache et al., 2019; Lovascio et al., 2017; Pai et al., 2009, 2010; Pancheshnyi et al., 2006; Pilla et al., 2006a; Xu et al., 2011). Various methods to generate non-equilibrium plasma are being explored and are progressing towards practical use including ignition of propane/air mixtures(Pancheshnyi et al., 2006) and stabilization of turbulent premixed flame(Pilla et al., 2006b, 2006a). However, the nanosecond pulsed discharges may face several issues, including non-uniform ignition, high energy consumption, electrode erosion, limited control over plasma parameters, heat management challenges, plasma stability problems, and delayed ignition.

Recently, microwave ignition has gained momentum as it potentially solves the problems faced by nanosecond pulsed ignition (Hwang et al., 2016; Ikeda et al., 2015; Ikeda & Ofosu, n.d.; Le et al., 2017; Padala, Nishiyama, et al., 2017; X. Zhang et al., 2021). Microwave ignition offers more uniform energy distribution, ensuring consistent ignition throughout the volume. It is more energy-efficient by coupling energy more effectively into the medium, reducing overall energy consumption. Since microwave discharges can operate without electrodes, they significantly reduce electrode erosion and maintenance needs. Additionally, microwaves allow for better control over plasma parameters, enabling precise tuning of the ignition process. They also distribute heat more evenly, mitigating thermal damage, and provide a more stable plasma environment, reducing fluctuations and ensuring reliable ignition. Moreover, microwave discharges can achieve immediate ignition, avoiding the delays seen with nanosecond pulses.

In this study, explore the ignition capability of our newly developed microwave igniter in pulse mode using 2.45 GHz microwaves (Le et al., 2019a, 2019b; Padala, Le, et al., 2017). This is a recent among several igniters developed throughout the years. Previously, a short microwave discharged igniter (MDI) (Ikeda et al., 2015; Le et al., 2017) has shown promise in mitigating igniter tip heating by separating the igniter to the transmitter through a hallow space called the resonating cavity. Only a ceramic tube holds the transmitter and the igniter together. Additionally, the system was miniaturized and made more efficient by using semiconductor elements. This technology has also shown promise in expanding the lean combustion limit and improving fuel efficiency with propane in real engine tests. We successfully generated an initial plasma source with a laser or spark plug, expanded it using microwaves, and maintained it in the atmosphere. Spectroscopic measurements confirmed the non-equilibrium state of the atmospheric pressure plasma at up to 10 atmospheres. However, the MDI's expensive parts are a major drawback when compared to common igniters. Thus, we shifted to a more economical flat spiral igniter as the igniter. This time, the transmitter and the igniter are attached together by a thin (1.2 mm diameter) Copper-Tungsten wire.

The goal of this study is to investigate the ignition capability of the flat igniter to generate plasma and achieve sustainable non-equilibrium plasma generation in the atmosphere. Transitioning the igniter materials from all metallic parts to ceramic spacers reduced potentially improves heating transfers and enhanced stability of ignition while expanding the lean limit. For continuous operation in actual machines, selecting heat-resistant, pressure-resistant, and wear-resistant materials and structures is crucial. Combustion improvement experiments in passenger car gasoline engines demonstrated excellent combustion characteristics. However, durability tests revealed wear issues during long-term operation.

To address this, we generated stable microwave plasma using a spiral tungsten igniter with ceramic spacer which assumably acts as a microwave resonating reflector, maintaining one directional plasma in space. Plasma characteristics were analyzed through spectroscopic measurements and high-speed camera.

Our current focus is on applying this technology to combustion ignition. A robust ignition source is needed to transition from an initial plasma source to a flame kernel and maintain continuous chemical reactions. We explore the plasma characteristics that facilitate this transition, achieving stable initial plasma and flame kernel formation in a short time. Unlike traditional spark plasma methods, our approach shows short breakdown points and sustained plasma in space with continuous microwave input.

Recent advancements in plasma-assisted combustion have led to systems enhancing ignition and extending lean burn limits in engines. Our work highlights a flat panel ignitor using microwave plasma, achieving an air-fuel ratio (A/F) of 31 in practical gasoline engine tests. Despite challenges with cost, the design emphasizes miniaturization and robustness for real-world applications.

2. Experimental Setup

A flat spiral igniter generates air plasma using microwave energy, as shown in Figure 1. The system includes a microwave source from i-Lab (Japan), a coaxial cable (SMA cable), a stub tuner for impedance matching (28-008, Maury Microwaves), and an SMA-connected flat spiral igniter mounted on a ceramic holder. High-speed camera monitoring using a Dantec Camera (Phantom) is employed to capture detailed plasma dynamics, with measurements conducted at a time resolution of 10μs and 8-bit depth, revealing three-dimensional plasma generation and non-equilibrium high-speed pulses expanding into space.

The ceramic holder, precisely measured at 35 mm in length, and the igniter, with an 8 mm diameter, are designed to optimize the study of microwave-induced air plasma generation. The coaxial cable

ensures efficient power transmission from the microwave source, while the stub tuner matches the impedance between the microwave source and the igniter, maximizing power transfer and plasma generation efficiency.
Spectroscopic measurements using Oriel Physics Czurny Turner Monochromator (MS257) under various conditions are used to assess the temperature-related non-equilibrium state of the plasma. These measurements provide insights into the characteristics and behavior of the plasma, enabling a comprehensive analysis of its properties and performance in different scenarios.

The high-speed camera captures the temporal evolution of the plasma, allowing for a detailed examination of its dynamics. This setup facilitates the study of microwave-induced air plasma generation, providing valuable data on the physical properties and potential applications of the plasma system.

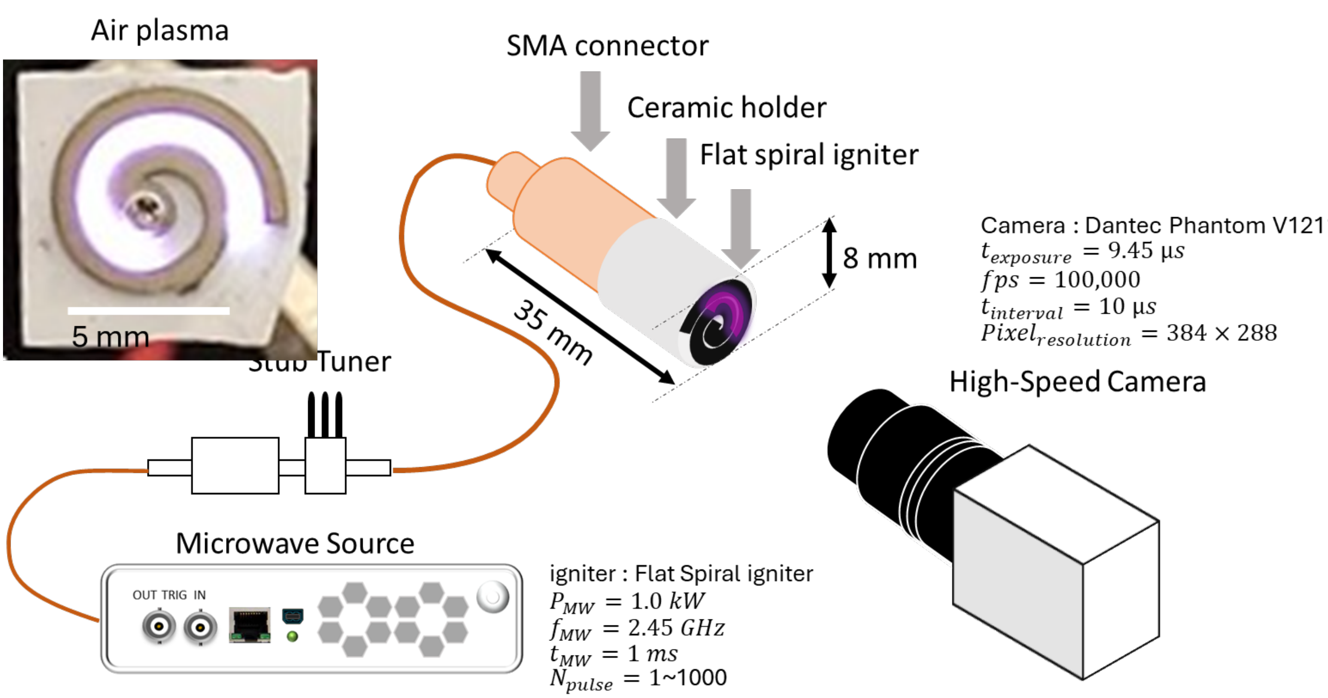

Figure 1. Schematic of the Plasma Generation System. The setup consists of a microwave source connected to a 35 mm flat igniter via an SMA connector. The igniter, held within a ceramic holder, features a flat spiral igniter with a diameter of 8 mm. The system is designed to induce plasma formation within the gaps of the spiral igniter.

2.1 High repetition frequency operations

In our ignition experiments, we used five different frequencies for higher repetition frequency operations as shown in Figure 2. At 100 KHz, we employed a pulse width of 1 μs and a period of 10 μs. For 20 KHz, the pulse width was 5 μs, with a period of 50 μs. At 10 KHz, the pulse width increased to 10 μs, and the period was 100 μs. For the 1 KHz frequency, we used a pulse width of 100 μs and a period of 1 ms. Finally, at 0.1 KHz (100 Hz), the pulse width was 1 ms, with a period of 10 ms. These pulse widths were defined by the maximum duty cycle of 10% permitted by the microwave semiconductor device. This systematic variation allowed us to optimize the ignition parameters and better understand the performance and efficiency under different pulsing regimes.

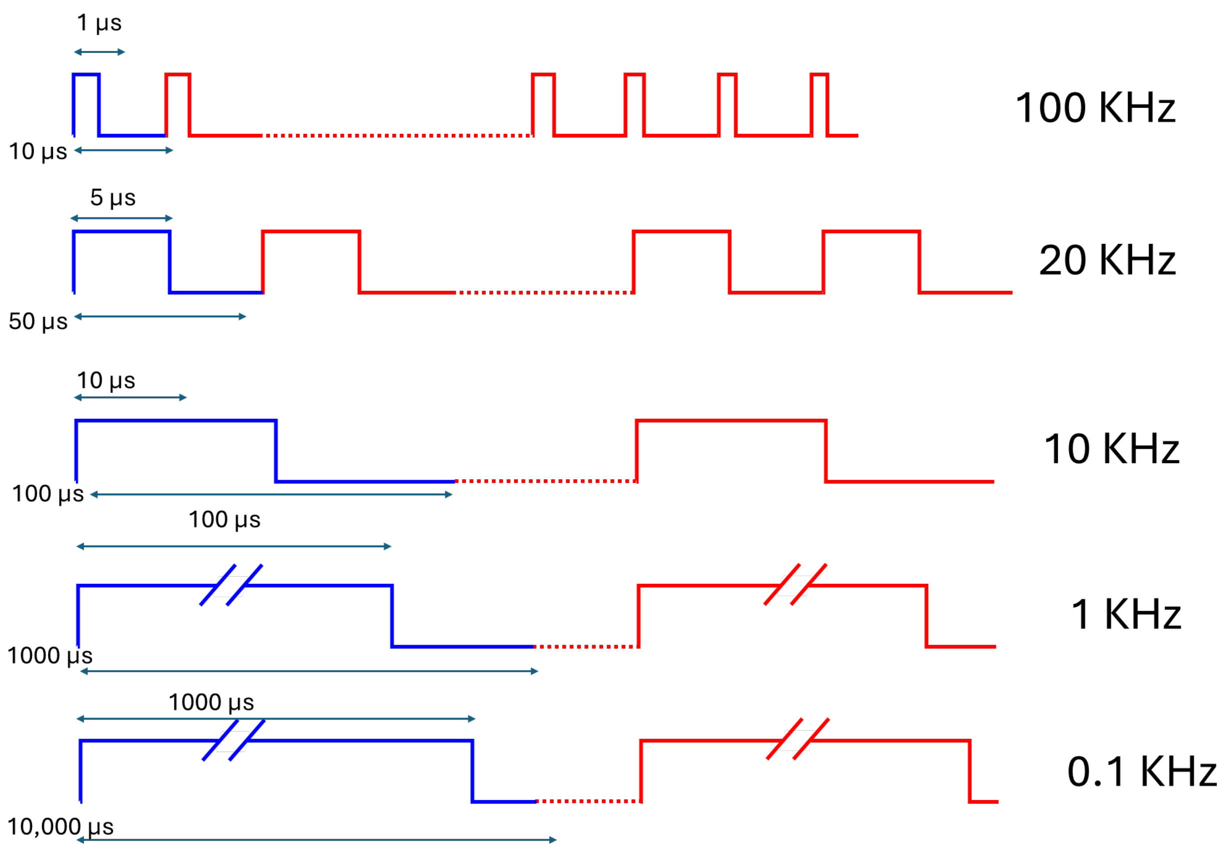

Figure. 2 Pulse widths used in each repetition frequency. Pulse widths and periods for different frequencies used in the ignition experiments. The pulse widths and periods are determined by the maximum duty cycle of 10% permitted by the microwave semiconductor device. At 100 KHz, the pulse width is 1 μs and the period is 10 μs. At 20 KHz, the pulse width is 5 μs and the period is 50 μs. At 10 KHz, the pulse width is 10 μs and the period is 100 μs. At 1 KHz, the pulse width is 100 μs and the period is 1 ms. At 0.1 KHz (100 Hz), the pulse width is 1 ms and the period is 10 ms. This variation in pulse width and period helps in optimizing the ignition parameters for different operational conditions.

2.2 Low repetition frequency operations

In our ignition experiments for low repetition frequency operations at 10 Hz, we utilized both long and short pulsed (burst mode) sequences to observe the evolution of plasma. For the long pulse mode, a single pulse with a width of 100 ms was used, followed by a period of 100 ms, ensuring a complete cycle of 1 second. This allowed us to study the plasma's behavior under sustained excitation.

In the short pulse mode, we employed a burst of shorter pulses, each with a width of 1 ms, within the same period of 100 ms. This burst consisted of a series of closely spaced pulses, enabling us to examine the plasma's response to rapid, repetitive excitation. The periods between these short pulses were 10 ms, maintaining the overall frequency of 10 Hz.

By comparing the plasma's behavior under these two different pulsing regimes, we gained insights into its dynamics and stability under varying conditions of excitation. The use of both long and short pulsed modes provided a comprehensive understanding of how different pulse widths and repetition frequencies affect the ignition and evolution of plasma.

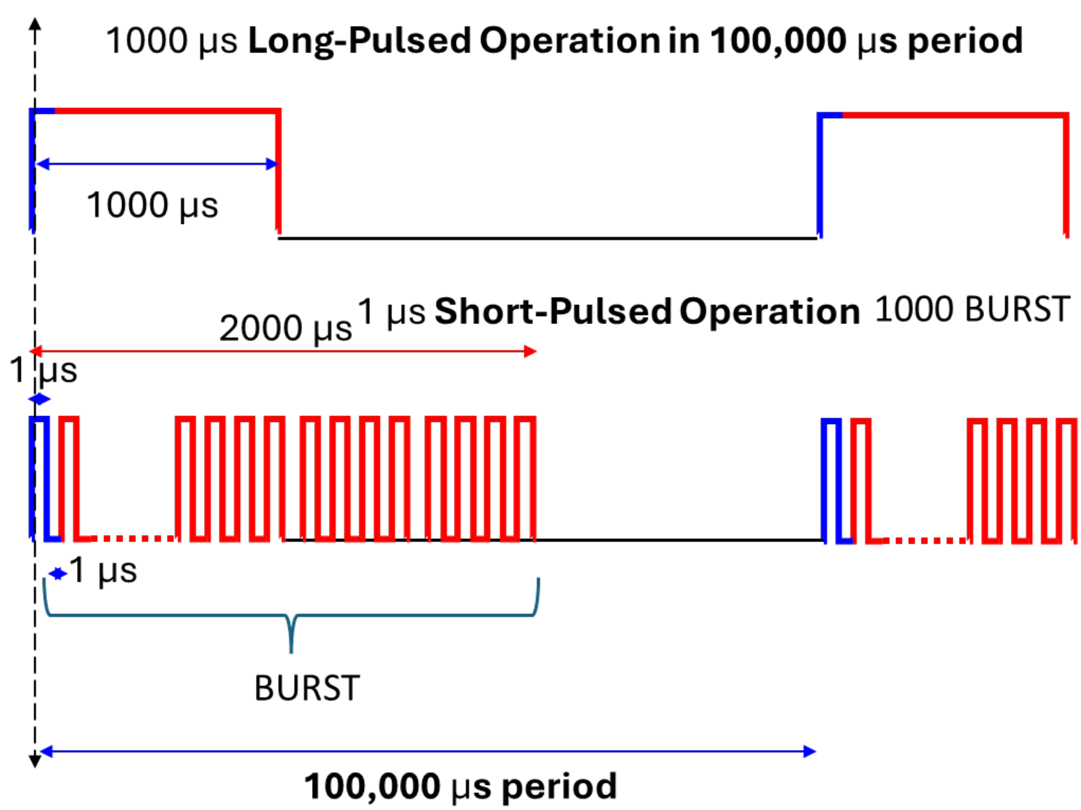

Figure. 3 Pulse sequences used in the low repetition frequency operation of 10 Hz. The long pulse mode employs a single pulse width of 100 ms with a period of 100 ms, resulting in a total cycle of 1 second. The short pulse

mode (burst mode) utilizes a burst of 1 ms pulses within the same 100 ms period, with intervals of 10 ms between pulses. These modes were used to observe the plasma's evolution under different excitation conditions.

3. Results

Whether in low or high repetition frequencies, successful ignition was observed under atmospheric air environment. The results are divided into three sections. The first section covers image and power measurements in high repetition frequency operations, where high-speed imaging techniques were used to capture detailed images of the plasma evolution, and power measurements were taken to assess the energy input and its effectiveness in sustaining the plasma. The second section focuses on high-speed imaging and power measurements in low repetition frequency operations, providing insights into the plasma's behavior and stability under different pulsing regimes. Finally, the third section discusses the plasma characteristics in both high and low repetition frequency operations, comparing the differences in plasma dynamics, stability, and overall performance under varying conditions.

3.1 High repetition frequency operations

Figure 2 shows the plasma image when the microwave transmission frequency is changed from 0.1 kHz to 100 kHz. The microwave is driven by a rectangular pulse. The initial energy jumps up to a peak of 1000 W and is maintained thereafter. The control is performed in 50 ns. The size of the plasma generated by the microwave changes slightly with the transmission frequency, but it does not seem to make much difference. The gap in the toroidal shape is about 1.2-1.4 mm, and the thickness is 1.0 mm. It is made of titanium. The signal from the semiconductor transmitter passes through a directional coupler and a stub tuner and is sent to a 10 mm coaxial part. The titanium part at the tip is connected to the coaxial part. At the beginning of the microwave transmission, a breakdown occurs in microseconds, and the microwaves thereafter maintain it. This image does not allow us to follow the time changes. The mechanism of microwave generation and plasma maintenance in high-speed video will be described later. Because the photo is black and white, the intensity and distribution of the plasma cannot be seen in detail. These will also be described later in high-speed video. The plasma image shown in Fig 1 is widely spread. This is the shooting time setting. More detailed characteristics will be described later.

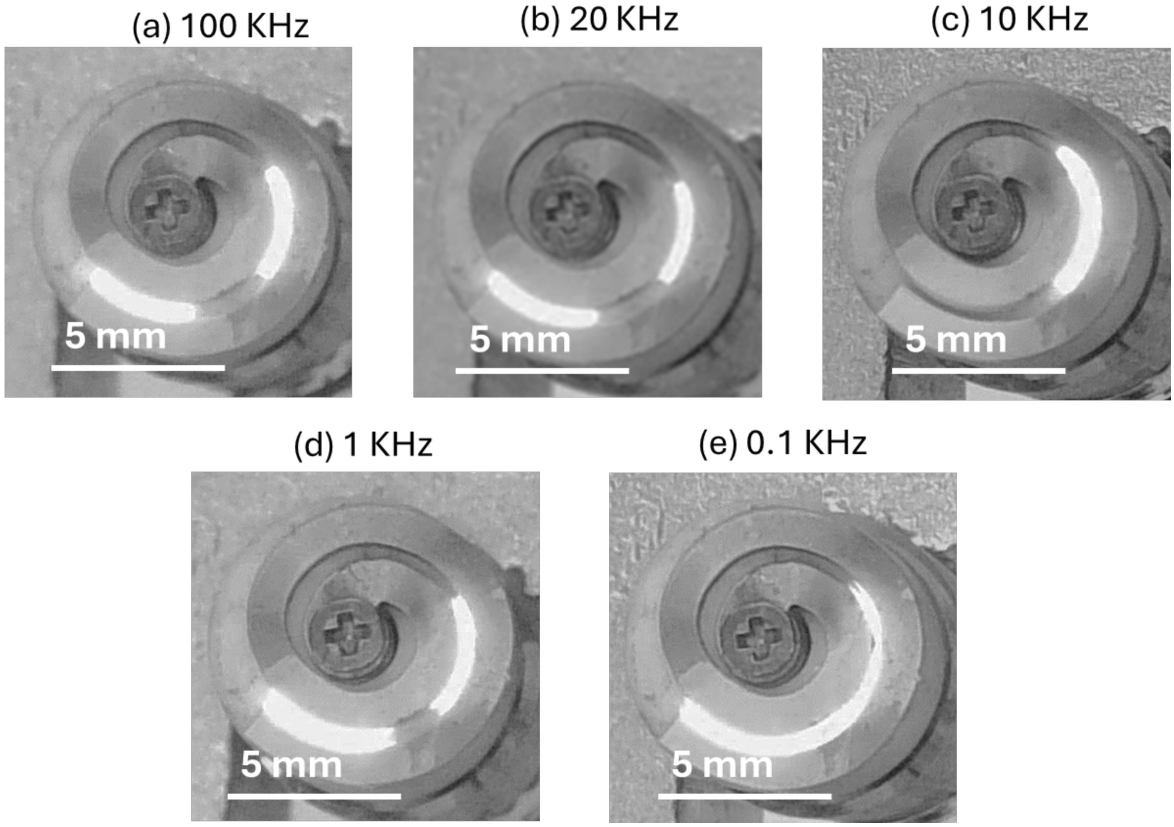

Figure 4. Effects of higher repetition frequency.

We have demonstrated with a LIBS system that plasma can be maintained in space by injecting microwaves after the initial plasma is formed. We have reported that the initial plasma can be expanded regardless of whether the pilot plasma is generated by a spark plug, a laser, thermal electrons, or microwaves.

The energy used to generate and maintain the initial plasma by microwaves is measured as a traveling wave and a reflected wave, and is shown in the figures. A microwave pulse of 1 microsecond takes 100-150 microseconds to rise. This phenomenon does not change even if the pulse width is changed to 1000 microseconds. The generation of the initial plasma by microwaves occurs in this 100-150 μs, and there is no significant difference in the level of the reflected wave. However, with a pulse of several hundred microseconds, it gradually decreases, dropping to 80%. However, there is no change in the level of reflection. The decrease in input energy contributes to the generation of the plasma as net energy. We believe that more than 95% of the input microwaves is used to generate the initial plasma. It can be seen that it takes about 3-4 microseconds even after the transmission is stopped. This is a characteristic of the microwave oscillator. This is a characteristic of microwave transmission systems. Temperature information is essential for the ignition source of combustion. Since we are discussing the equilibrium and non-equilibrium of plasma, we will proceed with the discussion on the plasma-like vibrational temperature, rotational temperature, and electron temperature, rather than gas temperature information. Before that, we will investigate the microwave input and reflected energy in these five types of launch patterns. We will investigate the plasma generation mechanism at the launch frequency.

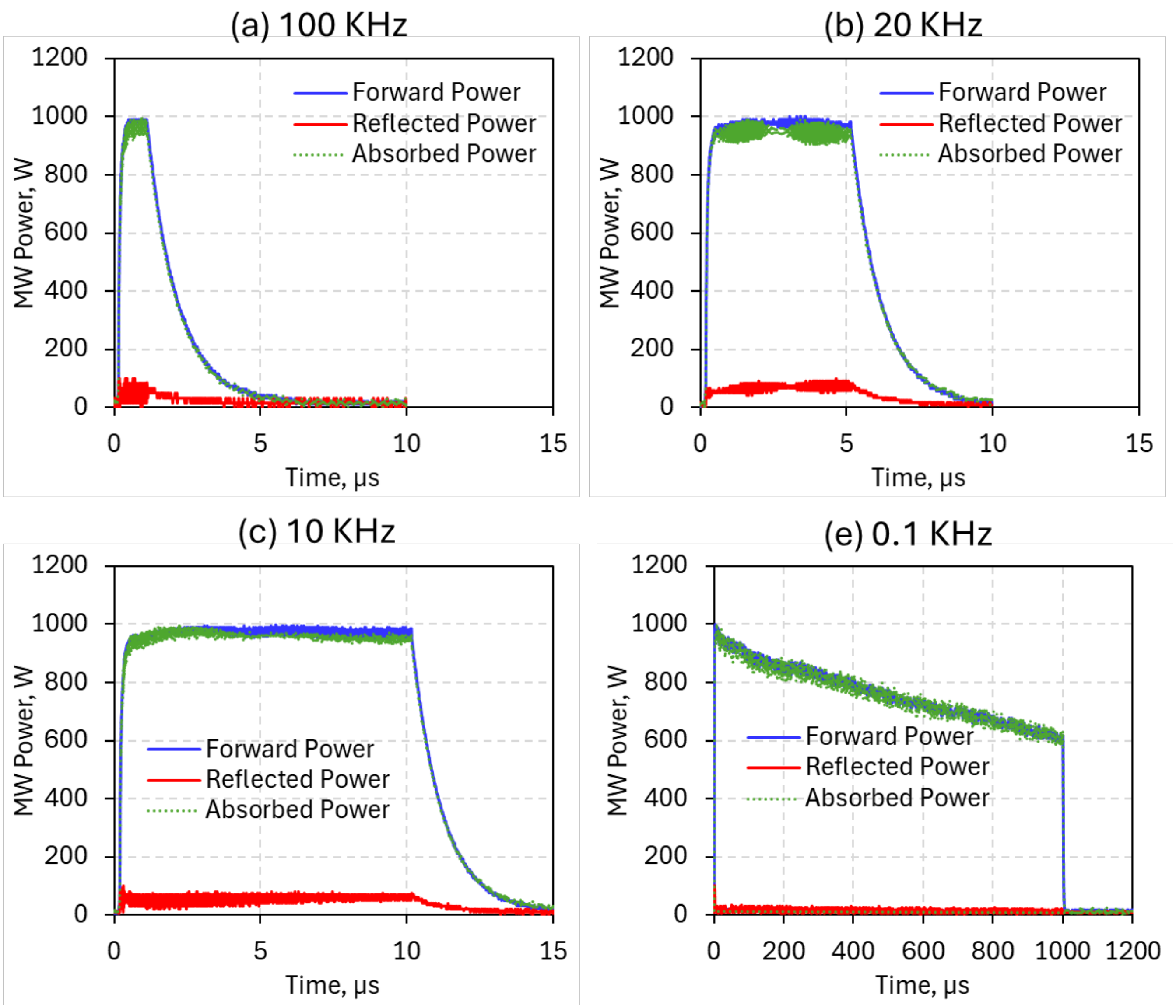

Figure 5. Power measurements in the varied high repetition frequency operations

3.2 Low repetition frequency operations

Microwave ignition systems feature two phases: the breakdown phase and the sustaining phase. The breakdown phase requires high power to ionize gas and create plasma, essential for starting combustion whicch depicted as a peak in the blue waveform in Figure 2. After plasma formation, the sustaining phase begins, where power is lowered to maintain the plasma and flame, illustrated by the shorter pulses in the red waveform. The transition from high "breakdown power" to lower "sustained power" is crucial, involving either continuous or pulsed waves, to optimize ignition efficiency and control. This results in better fuel efficiency, lower emissions, and improved performance compared to traditional ignition methods.

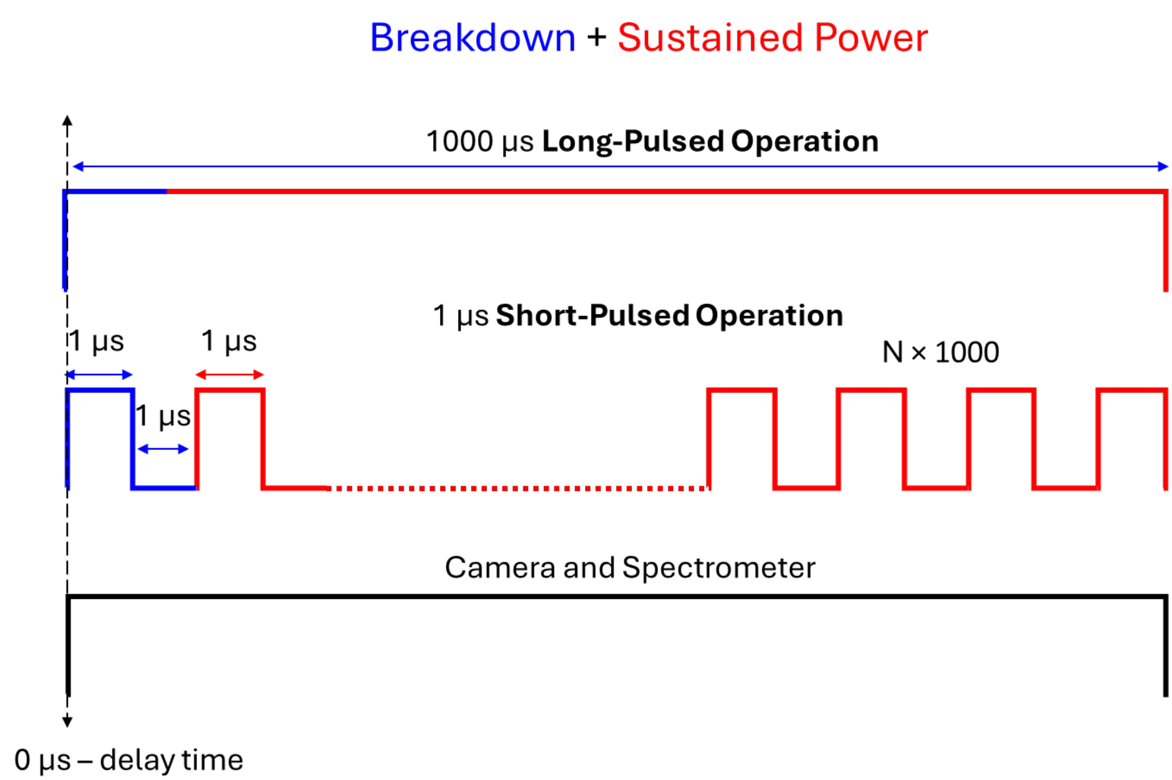

Figure 6. Power delivery profile for plasma generation. The diagram illustrates the two-stage microwave power application used in plasma formation.

The images are a time-series visualization of ignition and plasma formation, captured using a high-speed camera. The process captured is an instantaneous breakdown at 0 microseconds, where a spark is generated by a microwave igniter. This initial breakdown spark transitions into an discharge plasma, which then undergoes a dynamic change in size—first enlarging and then shrinking. At the beginning of the sequence, the plasma is at its nascent stage, indicated by a concentrated and intense coloration. As time progresses, plasma expands, reaching a maximum size before contracting. This plasma is sustained throughout the duration of the microwave pulse, which is delivered at a power of 1 kW and lasts until 1 millisecond (ms).

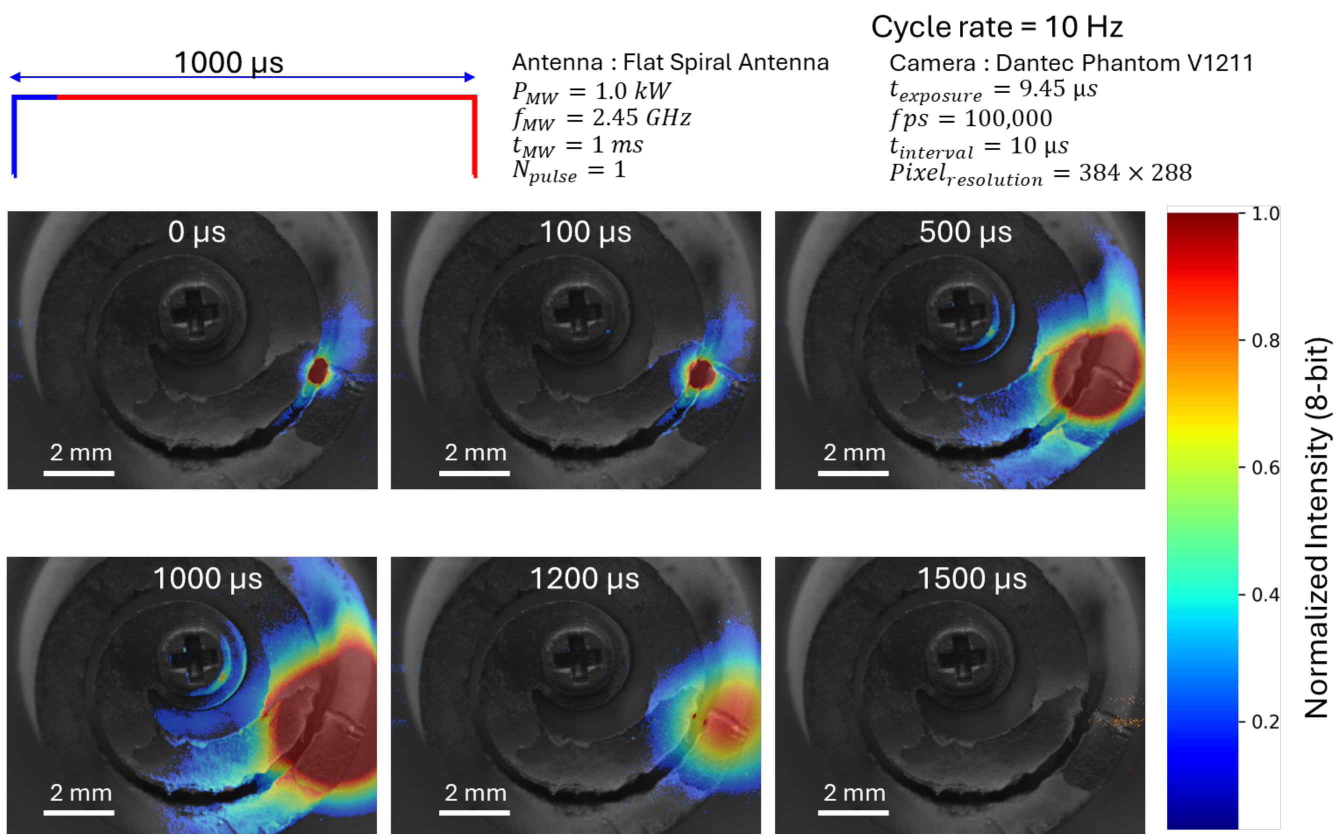

Figure 7. Time-series plasma formation using long-pulsed microwave.

The images depict the evolution of a glow discharge under conditions similar to long-pulsed operations. As the incandescent discharge tends to stabilize over time, we observed the glow discharge during the ~100th pulse. The sequence of images shows the discharge at various time intervals, starting from 0 μs up to 1030 μs. Initially, at 0 μs, the discharge is highly concentrated and intense. As time progresses, the discharge spreads and becomes more stable, with the intensity decreasing and the discharge area expanding.

At 10 μs, the discharge begins to show signs of spreading. By 30 μs and 40 μs, the discharge has expanded significantly, indicating a more stable glow. At 50 μs, the discharge continues to spread and stabilize. By 100 μs, the glow discharge covers a larger area with a more uniform intensity. At 200 μs and 400 μs, the discharge appears to be well-established and stable.
As we reach 800 μs, 1000 μs, 1010 μs, and finally 1030 μs, the discharge maintains its stability and shows a consistent glow pattern. The color bar on the right indicates the intensity of the discharge, with red representing the highest intensity and blue the lowest. These observations are crucial for understanding the stabilization and characteristics of the glow discharge under long-pulsed operations.

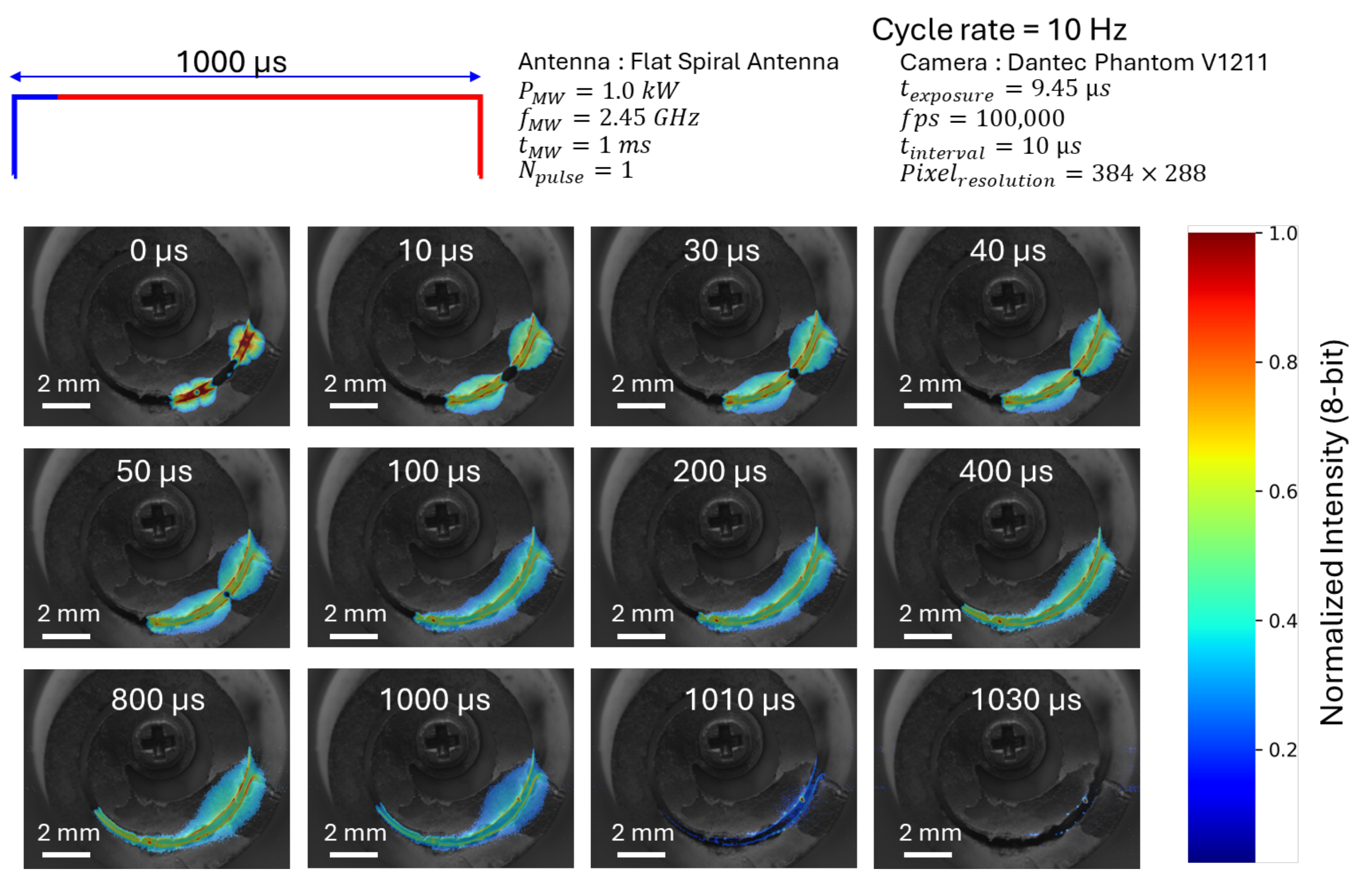

Figure 8. Time-series ignition of glow discharge in long pulsed operation.

The images depict the evolution of a glow discharge under the influence of short microwave (MW) pulses, in contrast to a long pulse that typically produces an incandescent plasma. At the first pulse, there is a brief formation of plasma which could exhibit incandescent characteristics. As the pulsing continues, by the 50th and 100th pulses, the images show that the plasma has transitioned to a stable glow discharge, evident from the more uniform and diffuse appearance in the heat map overlay. This is indicative of the plasma reaching a thermal equilibrium, where the energy provided by the microwave pulses is balanced by the losses to the surroundings.

With further pulsing at the 500th and 1000th intervals, the plasma appears to settle into a steady state, maintaining its glow without significant changes in intensity or size, suggesting that the process parameters have been well-tuned to sustain the discharge efficiently. After the last pulse, the residual heat signature of the plasma fades, confirming the cessation of energy input and the plasma's reliance on continuous pulsing to maintain its state.

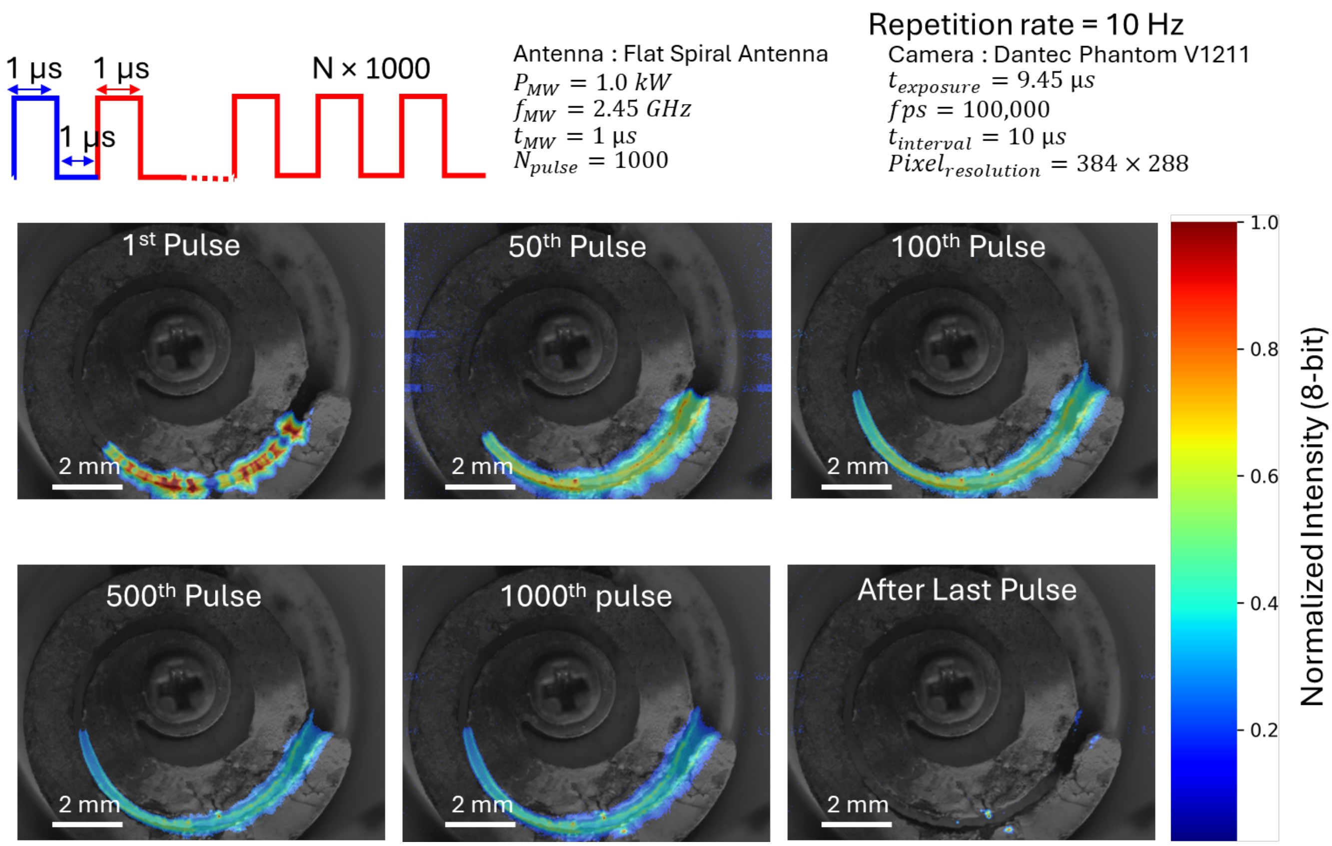

Figure 9. Time-series plasma formation using short-pulsed microwave.

As the system operates, several factors may contribute to the observed droop in Forward Power. The components in the microwave source and the transmission path, including the stub tuner, are subject to heating. This heat affects the material properties, altering the impedance and potentially causing a mismatch over time, which in turn can lead to a decrease in the forward power. This is because the temperature-dependent variations in impedance can reduce the effectiveness of the impedance match that was initially established. Additionally, the microwave power source may experience variations in output due to inherent characteristics or fluctuations in the power supply. Such variations, although typically minor, can result in changes in the delivered power. However, the graph indicates that any power droop present is relatively mild, implying that the system maintains a good impedance match and stability throughout the operation.

Reflected Power is depicted as low and consistent, reinforcing that the impedance matching is effective over the duration of the measurement. This low reflected power is indicative of a well-tuned system where minimal power is wasted. The Absorbed Power, deduced as the difference between the Forward and Reflected Power, is not directly measured but can be inferred to be significant, denoting that the igniter is effectively utilizing the majority of the power. This high absorption is favorable, as it signifies efficient ignition—a central aim in the design of microwave ignition systems.

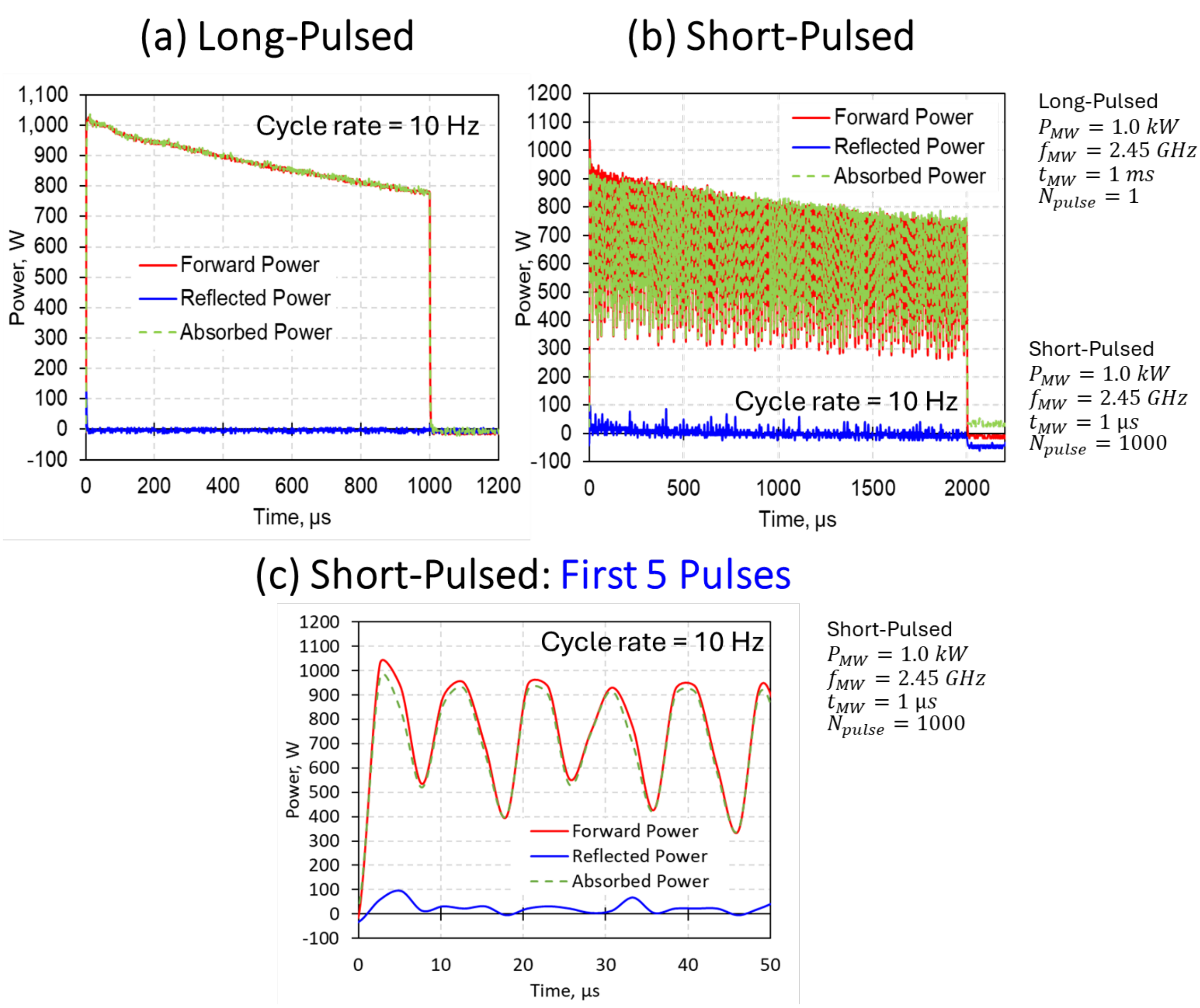

Figure 10. Power measurements during plasma formation.

The camera images were taken at 10 microsecond and 8-bit resolution. Let's see the time history of digitized plasma area. We apply 32 threshold intensity level in time history as shown in these figures. As seen in the image above, one or many plasmas were generated and expanded in the long pulse image. This can be seen from the left of the drawing. Microwaves were irradiated for 1000µs. During that time, the initial plasma gradually expanded. After the microwave irradiation, it suddenly contracted.

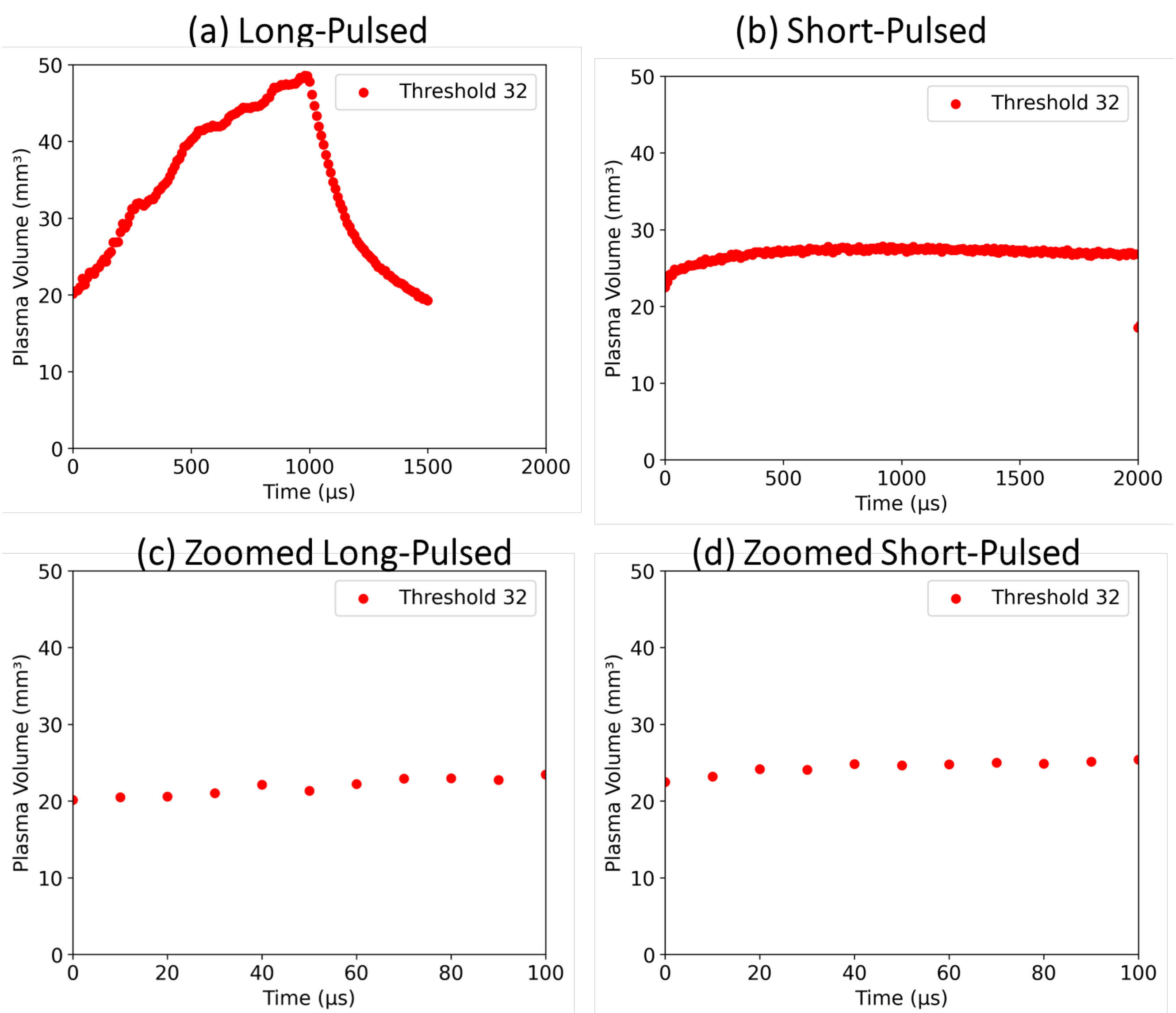

Figure 11. Volume expansion in (a) long and (b) pulsed operations.

This contraction is the same as in the previous presentation. In order to obtain two-dimensional information, we tried to see the change from the time and space changes of 8-bit information. The drawing shows information with the 255 level threshold of 8-bit changed to 50, 80, 100, 150, and 200. There is no significant difference in the characteristics of the time change. The time and tendency of the increase and disappearance after the plasma generation are the same. We will focus on the red line in the figure, 50/255, and proceed with the discussion.
Under short pulse conditions, several initial plasma nuclei are formed. An initial plasma is formed with one microwave energy, and it is maintained in time and space by the next pulse. It can also be seen that another plasma source is formed by another microwave. The volume of the plasma generated in large numbers also increases up to 200 μs after the initial pulse, and although there is no increase in volume thereafter, it is maintained for the time period. This phenomenon of maintenance is the same as with the long pulse. It is not possible to determine how many initial plasmas are formed, but at least in the image, the area is more than doubled. The area with the long pulse changes to the 3-30 mm3 level at 50/255. At this initial stage, it matches the 3-7 mm3 level with the short pulse. With the short pulse, it maintained a level of 6 mm3 even after attenuation over time. It is estimated that the volume of the plasma formed with the short pulse is almost the same as that generated at the beginning of the long pulse. In other words, there is no difference in the microwave plasma generation mechanism

Plasma temperature

The image displays simulated spectral emission profiles for the excited hydroxyl molecule (OH) and molecular nitrogen (N2) within a plasma environment, generated using SPECAIR software. This software predicts emission spectra based on molecular energy levels and transitions. The simulation is then compared with actual spectral data, with the goal of minimizing the residuals between them. The closest match provides estimates for the vibrational and rotational temperatures of the molecules involved.
For the long-pulsed plasma, there is a notable discrepancy between the simulated and actual spectral profiles for OH and N2. The inferred temperatures from these profiles exceed the 10,000 Kelvin limit of the SPECAIR simulations, suggesting that the real plasma temperatures may surpass the software's simulation capabilities. This implies that the actual plasma could possess higher energy than the simulations indicate.

Comparing the spectra of short-pulse plasma and long-pulse plasma shows that long-pulse plasma is almost a high-temperature thermal plasma. On the other hand, short-pulse plasma is a non-equilibrium plasma.

This is an important point to keep in mind when discussing the ignition phenomenon of various fuels in the future. We look forward to discussions on how thermal plasma and non-equilibrium plasma ignite and how the transition from the plasma source to the initialization region occurs.

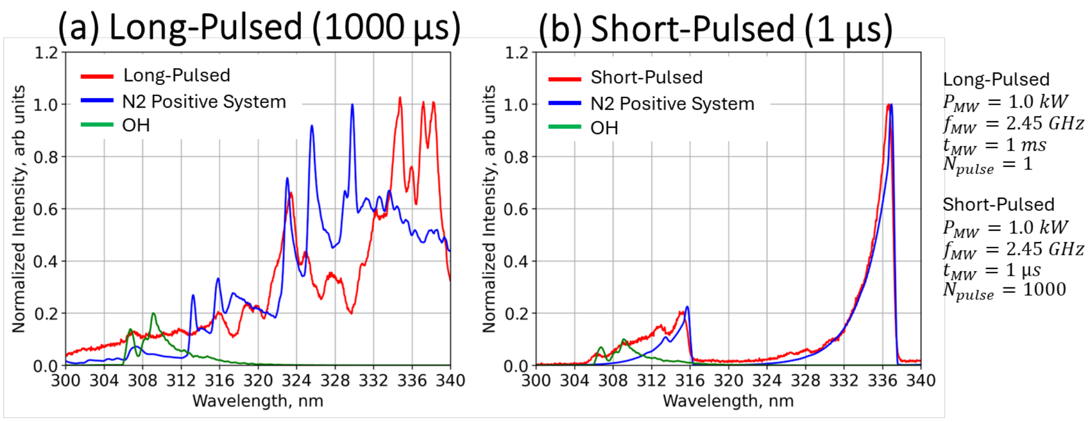

	Electron Temp	Vibrational Temp	Rotational Temp
Long-Pulsed	~14,000 K	~14,000 K	~14,000 K
Short-Pulsed	5,069 K	2,228 K	2,228 K

Figure 12. Temperature measurements using synthetic method.

Non-thermal characteristic dependence on frequency

Conversely, in the short-pulsed plasma condition, the actual spectral lines, depicted in red, closely match the simulated spectra. This strong correlation allows for more accurate derivation of the rotational and vibrational temperatures from the emission data. The temperatures obtained indicate a non-equilibrium state in the plasma: the vibrational temperature, which is a measure of the energy within molecular vibrations and impacts chemical reaction rates, is lower than the rotational temperature, which reflects the energy in molecular rotations corresponding to the gas's kinetic temperature. The distinction between these temperatures signifies the nonthermal characteristics of the plasma, with the implication that the molecular excitation is primarily rotational rather than vibrational.

The initial microwave energy is approximately 1mJ/pulse. Compared to the thermal plasma at 1000µs, we investigated the characteristics of the non-equilibrium plasma that is generated in large quantities. The spectroscopic spectrum is shown as the frequency is changed. This is a detailed spectrum of OH and N2P. This was converted to electron temperature, vibrational temperature, and rotational temperature and graphed. At all frequencies, the electron temperature is highest, followed by the vibrational temperature and then the rotational temperature. The existence of differences between these three temperatures indicates that this is a non-equilibrium plasma.

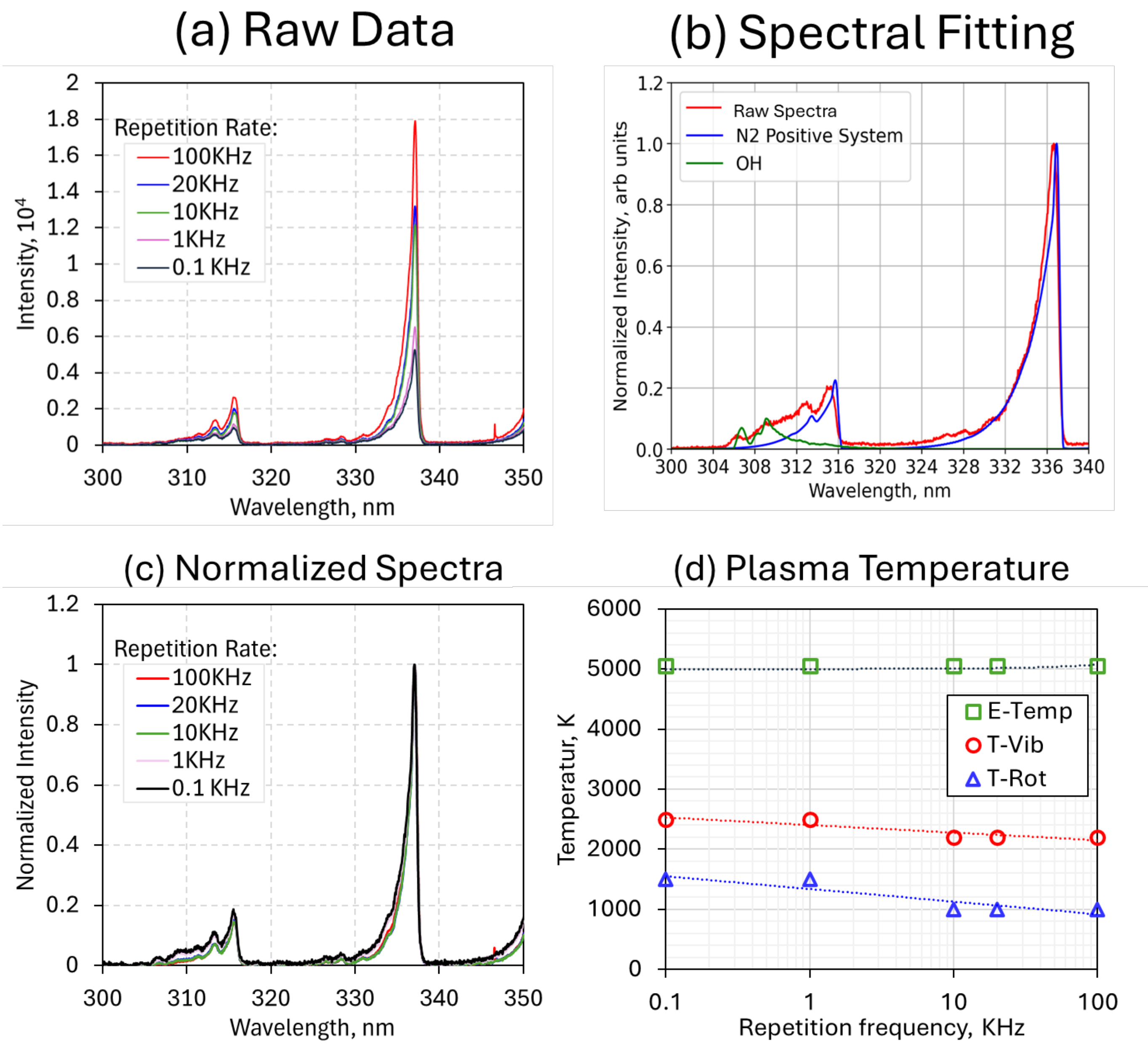

Figure 13. Spectral measurements in different high repetition frequency operations in (a) raw measured spectrum, (b) spectral fitted, (c) normalized spectrum. Finally, the plasma temperatures are plotted over fiffrent repetition frequency.

4. Conclusions

A cold equilibrium plasma source using microwave pulses has been developed. By changing the microwave transmission pattern, stable thermal plasma and non-equilibrium plasma maintained in the atmosphere were confirmed. With short-pulse microwave plasma transmission, non-equilibrium plasma is generated, and a certain plasma volume is formed in about 200 μs thereafter. On the other hand, under long-pulse conditions, after the initial plasma, the plasma deposition gradually expands to 2.5 times its size. Meanwhile, the temperature measured by spectroscopic measurement spectrum shows thermal plasma characteristics even for the vibrational and rotational temperatures. Regardless of the repetition frequency of the short pulse, the characteristics of non-equilibrium plasma are shown.

References

Akdoğan, E., & Şirin, H. T. (2021). Plasma surface modification strategies for the preparation of antibacterial biomaterials: A review of the recent literature. *Materials Science and Engineering: C*, *131*, 112474. https://doi.org/10.1016/J.MSEC.2021.112474

Bulat, M. P., Bulat, P. V., Denissenko, P. V., Esakov, I. I., Grachev, L. P., Volkov, K. N., & Volobuev, I. A. (2019). Ignition and combustion of air/fuel mixture in a long tube induced by microwave subcritical streamer discharge. *Acta Astronautica*, *163*, 33–43. https://doi.org/10.1016/j.actaastro.2019.01.028

Cheng, X., Zhang, X., Wang, Z., Wu, H., Wang, Z., & Chen, J. Y. (2021). Effect of microwave pulses on the morphology and development of spark-ignited flame kernel. *Energies*, *14*(19). https://doi.org/10.3390/en14196205

Dumitrache, C., Gallant, A., Minesi, N., Stepanyan, S., Stancu, G. D., & Laux, C. O. (2019). Hydrodynamic regimes induced by nanosecond pulsed discharges in air: mechanism of vorticity generation. *Journal of Physics D: Applied Physics*, *52*(36), 364001. https://doi.org/10.1088/1361-6463/ab28f9

Hwang, J., Bae, C., Park, J., Choe, W., Cha, J., & Woo, S. (2016). Microwave-assisted plasma ignition in a constant volume combustion chamber. *Combustion and Flame*, *167*, 86–96. https://doi.org/10.1016/j.combustflame.2016.02.023

Ikeda, Y., & Ofosu, J. A. (n.d.). Optimization of microwave discharge igniter for ignition enhancement: effect of microwave oscillation pattern on induced plasmas.

Ikeda, Y., Padala, S., Makita, M., & Nishiyama, A. (2015). Development of Innovative Microwave Plasma Ignition System with Compact Microwave Discharge Igniter. *SAE Technical Papers*, *2015*. https://doi.org/10.4271/2015-24-2434

Le, M. K., Nishiyama, A., & Ikeda, Y. (2019a). Evaluation of a novel miniaturised microwave resonating igniter: The Flat Panel Igniter. *Proceedings of the Combustion Institute*, *37*(4), 5613–5620. https://doi.org/10.1016/j.proci.2018.06.024

Le, M. K., Nishiyama, A., & Ikeda, Y. (2019b). Evaluation of a novel miniaturised microwave resonating igniter: The Flat Panel Igniter. *Proceedings of the Combustion Institute*, *37*(4), 5613–5620. https://doi.org/10.1016/j.proci.2018.06.024

Le, M. K., Padala, S., Nishiyama, A., & Ikeda, Y. (2017). Control of Microwave Plasma for Ignition Enhancement Using Microwave Discharge Igniter. *SAE Technical Papers*, *2017-September*. https://doi.org/10.4271/2017-24-0156

Lovascio, S., Ombrello, T., Hayashi, J., Stepanyan, S., Xu, D., Stancu, G. D., & Laux, C. O. (2017). Effects of pulsation frequency and energy deposition on ignition using nanosecond repetitively pulsed discharges. *Proceedings of the Combustion Institute*, *36*(3), 4079–4086. https://doi.org/10.1016/j.proci.2016.07.065

Ong, M. Y., Nomanbhay, S., Kusumo, F., & Show, P. L. (2022). Application of microwave plasma technology to convert carbon dioxide (CO2) into high value products: A review. *Journal of Cleaner Production*, *336*, 130447. https://doi.org/10.1016/J.JCLEPRO.2022.130447

Padala, S., Le, M. K., Nishiyama, A., & Ikeda, Y. (2017). Ignition of Propane-Air Mixtures by Miniaturized Resonating Microwave Flat-Panel Plasma Igniter. *SAE Technical Papers*, *2017-September*. https://doi.org/10.4271/2017-24-0150

Padala, S., Nishiyama, A., & Ikeda, Y. (2017). Flame size measurements of premixed propane-air mixtures ignited by microwave-enhanced plasma. *Proceedings of the Combustion Institute*, *36*(3), 4113–4119. https://doi.org/10.1016/j.proci.2016.06.168

Pai, D. Z., Lacoste, D. A., & Laux, C. O. (2010). Transitions between corona, glow, and spark regimes of nanosecond repetitively pulsed discharges in air at atmospheric pressure. *Journal of Applied Physics*, *107*(9). https://doi.org/10.1063/1.3309758

Pai, D. Z., Stancu, G. D., Lacoste, D. A., & Laux, C. O. (2009). Nanosecond repetitively pulsed discharges in air at atmospheric pressure—the glow regime. *Plasma Sources Science and Technology*, *18*(4), 045030. https://doi.org/10.1088/0963-0252/18/4/045030

Pancheshnyi, S. V., Lacoste, D. A., Bourdon, A., & Laux, C. O. (2006). Ignition of Propane–Air Mixtures by a Repetitively Pulsed Nanosecond Discharge. *IEEE Transactions on Plasma Science*, *34*(6), 2478–2487. https://doi.org/10.1109/TPS.2006.876421

Pilla, G., Galley, D., Lacoste, D. A., Lacas, F., Veynante, D., & Laux, C. O. (2006a). Stabilization of a Turbulent Premixed Flame Using a Nanosecond Repetitively Pulsed Plasma. *IEEE Transactions on Plasma Science*, *34*(6), 2471–2477. https://doi.org/10.1109/TPS.2006.886081

Pilla, G., Galley, D., Lacoste, D. A., Lacas, F., Veynante, D., & Laux, C. O. (2006b). Stabilization of a Turbulent Premixed Flame Using a Nanosecond Repetitively Pulsed Plasma. *IEEE Transactions on Plasma Science*, *34*(6), 2471–2477. https://doi.org/10.1109/TPS.2006.886081

Trinh, Q. H., Dinh, D. K., Lee, D. H., Nguyen, D. B., Mok, Y. S., & Lee, W. G. (2022). Combination of atmospheric pressure plasma with catalysts for dry reforming of methane to value-added chemicals. *Innovations in Thermochemical Technologies for Biofuel Processing*, 273–312. https://doi.org/10.1016/B978-0-323-85586-0.00009-3

Xu, D. A., Lacoste, D. A., Rusterholtz, D. L., Elias, P.-Q., Stancu, G. D., & Laux, C. O. (2011). Experimental study of the hydrodynamic expansion following a nanosecond repetitively pulsed discharge in air. *Applied Physics Letters*, *99*(12). https://doi.org/10.1063/1.3641413

Zhang, S., Chen, Z., Yang, J., Chen, S., Feng, D., Zhou, Y., Wang, B., & Lu, X. (2021). Study on discharge mode and transition mechanism of atmospheric pressure Ar/Zn pulsed microwave plasma jet. *AIP Advances*, *11*(9). https://doi.org/10.1063/5.0060269

Zhang, X., Wang, Z., Wu, H., Liu, C., Cheng, X., & Chen, J. Y. (2021). Propulsive effect of microwave-induced plasma jet on spark ignition of CO2-diluted CH4-air mixture. *Combustion and Flame*, *229*. https://doi.org/10.1016/j.combustflame.2021.111400

i-Lab. (n.d.). *Microwave enhanced system for LIBS*. Retrieved June 2024, from https://www.i-lab.net/english-here/new-product